

Accepted Manuscript

The inclusion complex of rosmarinic acid into beta-cyclodextrin: a thermodynamic and structural analysis by NMR and capillary electrophoresis

Amra Aksamija, Ange Polidori, Raphaël Plasson, Olivier Dangles, Valérie Tomao

PII: S0308-8146(16)30516-7

DOI: <http://dx.doi.org/10.1016/j.foodchem.2016.04.008>

Reference: FOCH 19015

To appear in: *Food Chemistry*

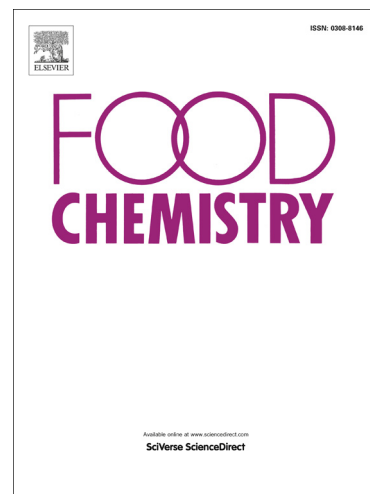
Received Date: 30 September 2015

Revised Date: 2 March 2016

Accepted Date: 4 April 2016

Please cite this article as: Aksamija, A., Polidori, A., Plasson, R., Dangles, O., Tomao, V., The inclusion complex of rosmarinic acid into beta-cyclodextrin: a thermodynamic and structural analysis by NMR and capillary electrophoresis, *Food Chemistry* (2016), doi: <http://dx.doi.org/10.1016/j.foodchem.2016.04.008>

This is a PDF file of an unedited manuscript that has been accepted for publication. As a service to our customers we are providing this early version of the manuscript. The manuscript will undergo copyediting, typesetting, and review of the resulting proof before it is published in its final form. Please note that during the production process errors may be discovered which could affect the content, and all legal disclaimers that apply to the journal pertain.



1 **The inclusion complex of rosmarinic acid into beta-cyclodextrin: a**
2 **thermodynamic and structural analysis by NMR and capillary**
3 **electrophoresis**

4

5

6 Amra Aksamija,^a Ange Polidori,^b Raphaël Plasson,^a Olivier Dangles,^a Valérie Tomao^{a*}

7

8

9

10 ^aUniversity of Avignon, INRA, UMR408 SQPOV, 84000 Avignon, France

11 ^bUniversity of Avignon, UMR5247 CBSA, 84000 Avignon, France

12

13

14

15

16

17 * Corresponding author.

18 E-mail address: valerie.tomao@univ-avignon.fr (V. Tomao).

19

20

21 **ABSTRACT**

22

23 This work focuses on the characterization of the rosmarinic acid (RA) - β -cyclodextrin (CD)
24 complex in aqueous solution by ^1H NMR (1D- and 2D-ROESY), completed with studies by
25 capillary electrophoresis (CE). From the ^1H NMR data, the stoichiometry of the complex was
26 determined by a Job's plot and the binding constant was estimated from a linear regression
27 (Scott's method). At pH 2.9, the results showed that RA binds CD with a 1:1 stoichiometry
28 and a binding constant K_b of $445 (\pm 53) \text{ M}^{-1}$ or $465 (\pm 81) \text{ M}^{-1}$ depending on the CD protons
29 (H-5 or H-3) selected for the evaluation. The K_b value was also calculated from the CD-
30 induced chemical shifts of each RA proton in order to collect information on the structure of
31 the complex.

32 The pH dependence of K_b revealed that the RA carboxylic form displays the highest affinity
33 for CD. An investigation by capillary electrophoresis fully confirmed these results. 2D
34 ROESY analysis provided detailed structural information on the complex and showed a
35 strong correlation between H-3 and H-5 of CD and most RA protons. In conclusion, RA, an
36 efficient phenolic antioxidant from rosemary with a marketing authorization, spontaneously
37 forms a relatively stable inclusion complex with CD in water.

38

39 **Keywords**

40 Beta-cyclodextrin, rosmarinic acid, inclusion complex, NMR, ROESY, capillary
41 electrophoresis

42

43 1. Introduction

44 Naturally occurring phenolic compounds are currently used in the food industry as additives,
45 especially in functional foods due to their potential health promotion in terms of antioxidant
46 and anti-inflammatory protection (Campos-Vega et al., 2010).

47 Rosmarinic acid (RA), an ester of caffeic acid and 3,4-dihydroxyphenyllactic acid, is a natural
48 phenolic compound commonly found in many Lamiaceae herbs such as *Rosmarinus*
49 *officinalis*, an aromatic evergreen shrub. Besides its antioxidant and anti-inflammatory
50 activities, RA has antiallergenic, antiviral, and antibacterial properties and displays a very low
51 toxicity (Petersen and Simmonds, 2003) and (Furtado et al., 2008). To fulfill the consumer
52 demand for natural food additives, rosemary extracts have been recently accepted by the EU
53 food additive legislation as effective and natural alternatives to synthetic antioxidants.

54 However, the effectiveness of these natural antioxidants depends on the preservation or
55 improvement of their stability, bioactivity and bioavailability (Fang and Bhandari, 2010).

56 Nano-encapsulation within food-grade macromolecules represents a remarkable mean to
57 maintain the structural integrity and potentially enhance the bioavailability of these bioactive
58 compounds (Munin and Edwards-Lévy, 2011). Cyclodextrins, a group of naturally occurring
59 macrocyclic oligosaccharides, are convenient encapsulating material widely used in the food
60 industry as additives for the stabilization of flavors and for the elimination of undesired tastes
61 (Astray et al., 2009). In particular, β -cyclodextrin (CD) has been listed as a safe food additive
62 since 1998 (Szente and Szejtli, 2004). Inclusion of natural phenols into CD enables their
63 protection against enzymatic oxidation and non-enzymatic oxidation by dioxygen and thus
64 can extend their stability over time (Cravotto et al., 2006).

65 Numerous analytical methods, such as spectroscopic, electrochemical or separation
66 techniques, have been used for the characterization of the inclusion complexes and the
67 estimation of the thermodynamic parameters of binding (Mura, 2014). Among these methods,
68 ^1H NMR is the most widely used (Pessine et al., 2012).

69 In aqueous solution, CDs are able to form inclusion complexes with a variety of phenolic
70 compounds such as hydroxytyrosol (López-García et al., 2010), baicalin (Li et al., 2009),
71 isoquercitrin (Wang et al., 2009), quercetin (Koontz et al., 2009), and caffeic acid (Zhang et
72 al., 2009). This ability is due to their cone-shaped structure with a relatively lipophilic inner
73 cavity and hydrophilic outer surface. The main driving force in complex formation is the
74 release of high-enthalpy water molecules from the CD cavity and the development of strong
75 van der Waals host (CD) – guest (ligand) interactions (Loftsson et al., 2005). Water molecules
76 are displaced by the more hydrophobic guest molecules with a concomitant decrease of CD
77 ring strain (Szejtli, 1998).

78 However, only few papers have been published on the inclusion of RA into CDs. Celik et al.
79 have studied the CD - RA binding and the corresponding changes in antioxidant capacity of
80 RA in solution using UV-visible and fluorescence spectroscopies (Celik et al. 2011).
81 Recently, Medronho et al. reported for the first time an NMR study of the β -CD - RA
82 interactions, giving insight on the complex structure (Medronho et al., 2014) ; however, much
83 higher values (by one order of magnitude) of the association constant were estimated in this
84 work.

85 These conflicting results prompted us to revisit CD – RA binding. As RA could be
86 encapsulated in CD for application in foods of variable acidity, we also investigated the pH-
87 dependence of the CD – RA binding to compare the affinity of the carboxylic and carboxylate
88 forms of RA for the macrocycle. In this work, the CD - RA inclusion complex (figure 1) was
89 investigated by 1D and 2D (ROESY) ^1H NMR in order to refine the structural
90 characterisation of the complex. Additionally, a complementary study by CE was performed.

91 The values of the binding constant (K_b) obtained by independent analytical tools (fluorescence
92 spectroscopy, NMR and CE) in different studies (Celik et al. 2011, Medronho et al. 2014 and
93 this work) will be discussed.

94 The experimental conditions for the formation of the inclusion complex are consistent with
95 the EU food additive legislation.

96

97 **2. Materials and methods**

98 *2.1 Materials*

99 Rosmarinic acid, caffeic acid (CA), sodium dihydrogenphosphate dihydrate and disodium
100 hydrogenphosphate heptahydrate were purchased from Sigma Aldrich (St. Louis, MO, USA).
101 β -Cyclodextrin was kindly given by Roquette Freres (Lestrem, France). Sodium hydroxide
102 was purchased from Prolabo (BDH Prolabo, VWR International, Haasrode, Belgium). Phenol
103 was obtained from Carlo Erba (Carlo Erba Reagents, SdS, Peypin, France). D₂O for NMR
104 analyses was purchased from Euriso-Top (Saint-Aubin, France). Demineralized water was
105 obtained from VWR (VWR International S.A.S, France). Standard solutions for capillary
106 conditioning, 0.1 M and 1.0 M NaOH solutions were supplied by Fluka Biochemika (Sigma-
107 Aldrich Chemie, GmbH, Steinheim, Germany) while milliQ water was produced by an EASY
108 pure RF compact ultrapure water system (Barnstead, ThermoFischer Scientific, Waltham, MA,
109 USA). All reagents were of analytical grade quality.

110 *2.2. NMR study*

111 All RA and CD solutions were freshly prepared in D₂O. For the Job's plot, different volumes
112 of 10 mM solutions of RA and CD in D₂O were mixed together to a constant volume keeping
113 the sum of the total RA and CD concentrations equal to 10 mM.

114 For the determination of the apparent association constant (Scott's plot), two different series
115 of samples were prepared.

116 In the first one, different volumes of a 1 mM CD solution in D₂O and of a solution containing
117 RA (10 mM) and CD (1 mM) in D₂O were mixed together to a constant volume with a final
118 RA/CD ratio ranging from 0.8 to 9.2.

119 In the second series, different volumes of a 1 mM RA solution and of a solution containing
120 CD (10 mM) and RA (1 mM) in D₂O were mixed together to a constant volume with a final
121 CD/RA ratio ranging from 0.8 to 9.2. Final solutions were equilibrated at room temperature
122 and protected from light before measurement.

123 1D ¹H NMR spectra were recorded on a Bruker AC-400 MHz spectrometer (software Bruker
124 Top Spin 2.1). 2D-ROESY spectra were recorded in on a Bruker AVL 600 MHz
125 (Spectropole, Aix-Marseille University).

126 Chemical shifts are given in ppm (δ) and calculated using the internal reference of the HDO
127 signal at 4.79 ppm. In all cases, the complexation-induced chemical shift difference is defined
128 as the difference between the chemical shift of the free molecule to the chemical shift of
129 bound molecule, $\Delta\delta = \delta_{\text{free}} - \delta_{\text{complex}}$.

130 *2.3 Capillary Electrophoresis study*

131 Electrophoresis experiments were performed using an automated capillary electrophoresis
132 system (Beckman P/ACE MDQ, Fullerton, CA). Fused-silica capillaries (50 μm i.d. \times 60 cm,
133 50 cm to the detector) were used.

134 Phosphate buffer (pH 7) for CE analysis was prepared with sodium dihydrogenphosphate
135 dihydrate and disodium hydrogenphosphate heptahydrate in milliQ water (ionic strength = 10
136 mM) and stored at 4°C. Working buffers were prepared by diluting up to 15 mM of CD in this
137 phosphate buffer.

138 Stock solutions of RA and CA, both in final concentration equal to 5 mM, were prepared in
139 milliQ water and protected from light at 4°C. Sodium thiosulphate (1 mM) was added to
140 protect the stock solutions against oxidation. Sonication of the stock solutions in an ultrasonic
141 bath (5 min) was necessary to achieve complete solubility. The stock RA and CA solutions
142 were renewed every 15 days. Samples for analysis were prepared by dilution of these stock
143 solutions in milliQ water. After dilution, the concentrations were 0.05 mM for RA, 0.2 mM
144 for CA and 1 mM for phenol.

145 Prior to first use, new capillaries were conditioned by flushing at 20 psi with milliQ water (2
146 min), 0.1 M NaOH (10 min), 1.0 M NaOH (5 min), milliQ water (2 min), then with working
147 buffer for 15 min. In order to remove potentially adsorbed analytes, the capillary was rinsed
148 with milliQ water (2 min), 0.1 M NaOH (5 min), milliQ water (2 min) and working buffer (5
149 min) every three consecutive runs. Before each sample run, the capillary was flushed with 0.1
150 M NaOH (1 min) and working buffer (5 min) and, after analysis, with working buffer (2 min).
151 The capillary was thermostated at 20 °C. The sample was injected in hydrodynamic mode at
152 0.5 psi for 5 s and each analysis was performed under an applied voltage of 10 kV. Any
153 measurement was repeated at least three times in identical conditions.

154

155 **3. Results and Discussion**

156 *3.1. Stoichiometry of the inclusion complex*

157 The stoichiometry of inclusion complex between RA and CD was determined by using the
158 method of continuous variations (Job's plot).

159 The CD protons that are most sensitive to bound RA are H-3 and H-5, as both points toward
160 the interior of the cavity. The significant diamagnetic shift observed for those protons is
161 essentially due to the magnetic anisotropy effects of RA's π -electrons in agreement with the
162 formation of an inclusion complex (Schneider et al, 1998; Ali and Upadhyay, 2008). Table S1
163 shows the chemical shifts differences of H-5 (CD) for a CD mole fraction (r_{CD}) ranging from
164 0.1 to 0.9. It is also noteworthy that the aromatic protons H-2, H-6, H2' and H-6' of RA are
165 also diamagnetically shifted. By contrast the other CD protons (H-1, H-2, H-4 and H-6),
166 mostly localized outside the CD cavity, experience insignificant chemical shift variations. The
167 superposition of the NMR spectra shows a significant shielding of the internal protons H-3
168 and H-5 of CD (figure 2). The stoichiometry of the inclusion complex was determined by
169 plotting $r_{CD} \times \Delta\delta$ (H-3, CD) against r_{CD} by using the Job's method (figure S1). The symmetry
170 of the curve obtained and its maximum at $r_{CD} = 0.5$ both point to a single complex of 1:1

171 stoichiometry. The same conclusion was reached with H-5. These results are in agreement
172 with previous investigations by fluorescence spectroscopy (Çelik et al., 2011) and NMR
173 (Medronho et al., 2014).

174 3.2. Stability of the inclusion complex

175 The apparent binding constant K_b was calculated according to the conventional Scott's
176 equation assuming 1:1 binding.

$$177 \frac{[RA]}{\Delta\delta_{obs}} = \frac{[RA]}{\Delta\delta_{max}} + \frac{1}{K_b\Delta\delta_{max}} \quad (1)$$

178 $\Delta\delta_{obs}$ represents the observed chemical shift difference of CD proton H-3 or H-5 between free
179 CD and the CD + RA mixtures. $\Delta\delta_{max}$ is the chemical shift difference at saturation. The
180 $[RA]/\Delta\delta_{obs}$ ratio for H-5 was plotted as a function of $[RA]$, thus resulting in an excellent linear
181 fit (figure 3). This confirms the 1:1 stoichiometry of the inclusion complex in agreement with
182 the Job's plot. From the slope of the plot, one obtains: $\Delta\delta_{max} = 0.22 \pm 0.01$ ppm. The same plot
183 with H-3 yields: $\Delta\delta_{max} = 0.10 \pm 0.01$ pm. The slope-to-intercept ratio equals the binding
184 constant. From the H-5 and H-3 plots respectively, one obtains: $K_b = 445 \pm 53$ M⁻¹ and $465 \pm$
185 81 M⁻¹. As expected, both values are identical within experimental error.

186 RA displays two phenolic rings and each of them may be involved in the binding. A second
187 series of measurements, in which RA is in low and constant concentration (1 mM) and CD in
188 variable concentration, was performed to collect information on the structure of the complex.
189 Although the CD-induced chemical shift displacements of the RA protons are weak, Scott's
190 plots could be constructed to estimate $\Delta\delta_c$ and K_b . The K_b values thus obtained are slight
191 lower than the one obtained by monitoring the CD protons (Table S2). The latter are
192 considered more reliable based on the higher sensitivity of the CD protons (especially H-5) to
193 RA-CD binding, which is obvious from the larger $\Delta\delta_{max}$ values.

194 3.3. Structure of the inclusion complex

195 The assignments of RA protons were made on the basis of their specific coupling constants
196 and on the COSY spectrum. The complete ¹H-NMR data for each of RA protons is presented

197 in the Table S3 and is consistent with those previously obtained in the literature (Lecomte et
198 al, 2010). Analysis of the NMR spectrum of RA (1 mM) shows signals of six aromatic
199 protons (H-2, H-5, H-6 and H-2', H-5', H-6'), two vinylic protons (H-7, H-8) and three
200 aliphatic protons (H7'_a, H7'_b and H-8').

201 In figure S2, the ¹H NMR data show the large variations induced by RA on the chemical
202 shifts of the CD protons located inside the cavity (H-3, H-5), compared with the weak
203 variations of the CD protons located outside (H-1, H-2, H-4). Upon complex formation, the
204 large shielding of H-3 and H-5 reflects the presence of one of the RA aromatic rings in the
205 CD cavity.

206 In figure S3, the ¹H NMR data of free and bound RA are compared. Maximal CD-induced
207 deshielding occurs for aromatic protons.

208 The geometry of the RA-CD complex was further investigated via a ROESY experiment.
209 Two different mixing times were used to obtain the NOE correlations between RA (350 ms)
210 and CD (150 ms) (figure 4). As expected from the 1D NMR spectra, strong correlations were
211 observed between the CD H-3 and H-5 protons on the one hand and most of the RA protons
212 on the other hand, especially H-2' and H-5' but also H-2. No correlation was observed
213 between the RA protons and the protons of the CD outer surface (H-2, H-4). These results
214 confirm without ambiguity the encapsulation of RA inside the CD cavity. The correlations
215 between the CD protons and all RA aromatic protons suggest that both phenolic moieties can
216 interact with the CD cavity. It can thus be assumed that two inclusion complexes are formed,
217 one involving the caffeoyl moiety (complex 1, binding constant K_1) and the other one
218 involving the 3,4-dihydroxyphenyllactic moiety (complex 2, binding constant K_2), both being
219 in fast equilibrium via free RA. Overall, only a single averaged NMR spectrum is observed
220 for the three species.

221 The observed chemical shift of any RA proton can be expressed as: $\delta_{\text{obs}} = x_0\delta_0 + x_1\delta_1 + x_2\delta_2$,
222 δ_0 , δ_1 and δ_2 being the chemical shifts of the proton in free RA, complex 1 and complex 2,
223 respectively, and x_0 , x_1 and x_2 the corresponding mole fractions.

224 Simple solution chemistry gives:

$$225 \quad \delta_{\text{obs}} = \frac{\delta_0 + (\delta_1 K_1 + \delta_2 K_2)[CD]}{1 + (K_1 + K_2)[CD]} = \frac{\delta_0 + \delta_{\text{max}} K_b [CD]}{1 + K_b [CD]} \quad (2)$$

$$226 \quad \text{With } K_b = K_1 + K_2 \text{ and } \delta_{\text{max}} = \frac{\delta_1 K_1 + \delta_2 K_2}{K_1 + K_2}$$

227 Therefore, whatever the proton signal detected, the apparent binding constant derived from
228 the chemical shift variations is the same and equals the sum of the individual binding
229 constants. It can thus be assumed that differences in K_b values depending on the RA proton
230 detected merely reflect differences in sensitivity.

231 However, it can be noted that the NOE correlations are especially intense between with the
232 CD H-3 and H-5 protons and the vinylic protons of the caffeoyl part, which suggests a deep
233 inclusion of this moiety into the cavity.

234 3.4. pH dependence of binding

235 The pH-dependence of the CD-RA complexation was investigated. At pH 2.9, RA is a
236 mixture of neutral carboxylic (RA-CO₂H) and anionic carboxylate (RA-CO₂⁻) forms in nearly
237 equal proportions. When the pH was decreased to 1 (pure RA-CO₂H), the K_b values deduced
238 from Scott's plots for the RA protons (variable CD concentration) were significantly higher.
239 By contrast, when the pH was increased to 6 (pure RA-CO₂⁻), the K_b values were lower.

240 Clearly, the less hydrophilic carboxyl form display a higher affinity for the CD cavity than the
241 corresponding carboxylate. On the other hand, at pH 1 and 6, the Job's plots confirmed the
242 1:1 stoichiometry of the inclusion complex (data not shown). As shown in table 1, the K_b
243 values obtained at pH 6 (*ca.* 200 M⁻¹) are of the same order of magnitude as those obtained by
244 Celik et al. (164 M⁻¹) by fluorescence but much lower than those obtained by Medronho et al.
245 by NMR. Indeed, at pH 6, Medronho et al. have estimated K_b at *ca.* 1180 M⁻¹ and 2030 M⁻¹

246 depending on which RA aromatic ring is monitored and interpreted this difference by
247 assuming two complexes in solution, the first one involving the caffeoyl moiety and the
248 second the 3,4-dihydroxyphenyllactic moiety. As stated above, this interpretation is incorrect
249 as both complexes are indistinguishable by NMR due to fast chemical exchange. Hence,
250 differences in K_b values must be ascribed to differences in sensitivity depending on the
251 protons monitored and techniques adopted (detection on RA at variable CD concentration vs.
252 detection on CD at variable RA concentration).

253 3.5 Analysis of RA-CD inclusion complexes by capillary electrophoresis

254 To confirm the NMR data, the RA-CD inclusion complex was also studied by CE. The
255 electrophoretic mobility of RA was measured in buffered CD solutions at different
256 concentrations (Li and Waldran, 1999). The binding kinetics being fast with respect to the
257 separation time, the measured mobility μ is the average mobility of the free (μ_{RA}) and bound
258 (μ_{RA-CD}) RA forms:

$$259 \quad \mu = (1 - \alpha) \cdot \mu_{RA} + \alpha \cdot \mu_{RA-CD} \quad (3)$$

260 α being the bound fraction of RA. For a large CD-to-RA molar ratio, the free CD
261 concentration can be considered constant and equal to the total CD concentration C , so that
262 the binding constant can be expressed as:

$$263 \quad K_b = \frac{[RA-CD]}{[RA][CD]} = \frac{\alpha}{(1-\alpha) \cdot C} \quad (4)$$

264 Hence, the measured electrophoretic mobility can be expressed as a function of C :

$$265 \quad \mu = \frac{\mu_{RA} + K_b C \cdot \mu_{RA-CD}}{1 + K_b C} \quad (5)$$

266 On top of binding effects, an increase in CD concentration leads to an increase in the buffer
267 viscosity (Paduano et al., 1990), and this in turn influences all the electrophoretic mobilities,
268 which are inversely proportional to the buffer viscosity (Plasson and Cottet 2005). The
269 electroosmotic flow μ_{eof} being inversely proportional to the buffer viscosity too (Corradini
270 and Spreccacenero, 2003), it was used for evaluating the viscosity correction factor to be
271 applied to the measured electrophoretic mobilities (Li and Waldran, 1999). A linear

272 relationship between the elution time of a neutral marker (phenol) t_{eof} and the CD
273 concentration was observed (correlation coefficient $R = 0.92$). It corresponds to a linear
274 variation of the viscosity with a maximal variation of 8% for a CD concentration of 15 mM.

275 The K_b values can be obtained from the non-linear curve-fitting of the plot expressing the
276 viscosity-corrected electrophoretic mobility μ as a function of C according to eq. (5), thus
277 enabling the determination of the numerical values of μ_{RA} , μ_{RA-CD} and K_b . The same method
278 was repeated with caffeic acid (CA) for comparison purposes, as CA is structurally related to
279 RA (see figure 1). The measurements were performed at 20 °C. The pH was fixed at 7 so as to
280 ensure that the carboxyl groups of RA and CA are fully deprotonated. The ionic strength was
281 fixed to a low value of 10 mM in order to avoid any heating of the capillary. Moreover, in
282 those conditions, the ionic and actual electrophoretic mobilities can be taken equal (Plasson
283 and Cottet, 2005).

284 The non-linear curve fitting yields: $K_b = 197 (\pm 14) M^{-1}$, $\mu_{RA} = 1.520 (\pm 0.006) \times 10^{-8} m^2V^{-1}s^{-1}$
285 and $\mu_{RA-CD} = 0.934 (\pm 0.014) \times 10^{-8} m^2V^{-1}s^{-1}$ for RA, $K_b = 176 (\pm 4) M^{-1}$, $\mu_{CA} = 2.101 (\pm$
286 $0.003) \times 10^{-8} m^2V^{-1}s^{-1}$ and $\mu_{CA-CD} = 1.047 (\pm 0.014) \times 10^{-8} m^2V^{-1}s^{-1}$ for CA (see figure 5).

287 The similar K_b values for RA and CA suggest that the caffeoyl moiety of RA is mostly
288 responsible for the affinity of RA for CD and that the less polarizable dihydroxyphenyllactic
289 moiety experiences a weaker binding. Taking hydroxytyrosol as a structural analog of the
290 dihydroxyphenyllactic moiety, it can actually be noted that this olive phenol only weakly
291 binds CD with a K_b value of *ca.* $90 M^{-1}$ (López-García et al., 2010).

292 The electrophoretic mobilities can also be used to evaluate the hydrodynamic radius of each
293 species (Plasson and Cottet, 2005):

$$294 \quad r_i = \frac{q}{6\pi\eta\mu_i} \quad (6)$$

295 with q the electric charge of the compounds (1.6×10^{-19} C) and η the water viscosity at 20 °C
296 (10^{-3} Pa.s). This gives $r_{RA} = 5.6 \text{ \AA}$, $r_{CA} = 4.0 \text{ \AA}$, $r_{RA-CD} = 9.1 \text{ \AA}$, $r_{CA-CD} = 8.1 \text{ \AA}$. These values can
297 be compared with the hydrodynamic value of β -CD: $r_{CD} = 7.7 \text{ \AA}$ (Pavlov *et al.* 2010). They

298 are consistent with the inclusion of either RA or CA inside the β -CD cavity, as evidenced by a
299 slight radius increase from free β -CD to the CA- β -CD and RA- β -CD complexes.

300 Close K_b values are thus obtained for RA- β -CD with this method and with the NMR method
301 in neutral conditions (about 200 M^{-1} , see Table 1) with a similar precision (about 10% error).

302 This value is also in good agreement with the one determined by Celik et al. by fluorescence
303 ($164 \pm 65 \text{ M}^{-1}$) rather than with the value obtained by NMR by Medrohno et al. (ca. 2000 M^{-1}).
304 The consistency of EC methods with fluorescence methods was furthermore checked by
305 performing a similar study for the association of RA with methyl- β -CD. A K_b value of $372 (\pm$
306 $20) \text{ M}^{-1}$ was determined; once again, this value is in perfect agreement with the value
307 measured by Celik *et al.* ($328 \pm 39 \text{ M}^{-1}$).

308

309 **4. Conclusion**

310 The complementary use of 1D and 2D ROESY NMR and EC methods have led to consistent
311 results concerning the complex formation between RA and β -CD. In all conditions, a mixture
312 of 1:1 complexes in fast equilibrium was obtained, both catechol subunits of RA being
313 potentially inserted inside the CD hydrophobic cavity, while no interactions of RA with the
314 outside of the CD unit could be reliably detected. Typically, the apparent binding constant is
315 ca. 450 M^{-1} at pH 2.9 (equimolar mixture of the carboxyl and carboxylate forms),
316 corresponding to an encapsulation efficiency of ca. 50% when the two species are mixed in an
317 equimolar concentration of 5 mM each. The pH dependence of K_b shows that the carboxyl
318 form of RA displays a higher affinity for the macrocycle than the carboxylate form.

319 In conclusion, RA forms a relatively stable complex with β -CD, especially in acidic
320 conditions. By accommodating the catechol nuclei inside the CD cavity, the binding could
321 inhibit their interactions with redox-active metal traces, thereby providing higher stability for
322 food applications. The binding could also modulate the release of RA in the digestive tract as
323 a function of pH.

324

325 **Acknowledgements**

326 The authors thank Roquette Freres (Lestrem, France) for providing β -cyclodextrin.

327

328 **Appendix. Supplementary data**

329 Supplementary data associated with this article can be found in Appendix.

330

331 **References**

332

333 Ali, S. M., Upadhyay, S. K. (2008). Complexation studies of pioglitazone hydrochloride and
334 β -cyclodextrin: NMR (^1H , ROESY) spectroscopic study in solution. *Journal of Inclusion*
335 *Phenomena and Macrocyclic Chemistry*, 62, 161-165.

336 Astray, G., Gonzalez-Barreiro, C., Mejuto, J.C., Rial-Otero, R., Simal-Gándara, J. (2009). A
337 review on the use of cyclodextrins in foods. *Food Hydrocoll.*, 23, 1631-1640.

338 Çelik, S.E., Özyürek, M., Tufan, A.N., Güçlü, K., Apak, R. (2011). Spectroscopic study and
339 antioxidant properties of the inclusion complexes of rosmarinic acid with natural and
340 derivative cyclodextrins. *Spectrochim. Acta. A. Mol. Biomol. Spectrosc.*, 78, 1615-1624.

341 Corradini, D., and Spreccacenero, L. (2003). Dependence of the Electroosmotic Flow in Bare
342 Fused-Silica Capillaries from pH, Ionic Strength and Composition of Electrolyte Solutions
343 Tailored for Protein Capillary Zone Electrophoresis. *Chromatographia*, 58, 587-596.

344 Cravotto, G., Binello, A., Baranelli, E., Carraro, P., Trotta, F. (2006). Cyclodextrins as Food
345 Additives and in Food Processing, *Current Nutrition and Food Science*, 2, 343-350.

346 Fang, Z., Bhandari, B. (2010). Encapsulation of polyphenols. *Trends Food Sci. Technol.*, 21,
347 510-523.

348 Furtado, M.A., de Almeida, L.C.F., Furtado, R.A., Cunha, W.R., Tavares, D.C. (2008).
349 Antimutagenicity of rosmarinic acid in Swiss mice evaluated by the micronucleus assay.

- 350 *Mutat. Res.*, 657, 150-154.
- 351 Koontz, J. L., Marcy, J. E., O'Keefe, S. F., Duncan, S. E. (2009). Cyclodextrin Inclusion
352 Complex Formation and Solid-State Characterization of the Natural Antioxidants α -
353 Tocopherol and Quercetin. *J. Agric. Food Chem.*, 57, 1162-1171.
- 354 Lecomte, J., Giraldo López, L.J., Laguerre, M., Baréa, B., Villeneuve P. (2010). Synthesis,
355 Characterisation and Free Radical Scavenging Properties of Rosmarinic Acid Fatty Esters.
356 *Journal of the American Oil Chemists Society*, 87, 615-620.
- 357 Li, J., and Waldron, K.C. (1999). Estimation of the pH-independent binding constants
358 of alanylphenylalanine and leucylphenylalanine stereoisomers with β -cyclodextrin in the
359 presence of urea. *Electrophoresis*, 20, 171-179.
- 360 Li, J., Zhang M., Chao, J., Shuang, S. (2009). Preparation and characterization of the
361 inclusion complex of Baicalin (BG) with β -CD and HP- β -CD in solution: An antioxidant
362 ability study. *Spectrochimica Acta Part A*, 73, 789-793.
- 363 Loftsson, T., Jarho, P., Másson, M., Järvinen, T. (2005). Cyclodextrins in drug delivery.
364 *Expert Opin. Drug Deliv.*, 2, 335-351.
- 365 López-García, M.Á., López, Ó. Maya, I., Fernández-Bolaños, J.G. (2010). Complexation of
366 hydroxytyrosol with β -cyclodextrins. An efficient photoprotection. *Tetrahedron*, 66, 8006-
367 8011.
- 368 Munin, A., Edwards-Lévy, F. (2011). Encapsulation of Natural Polyphenolic Compounds.
369 *Pharmaceutics* 3, 793-829.
- 370 Mura, P., n.d. Analytical techniques for characterization of cyclodextrin complexes in
371 aqueous solution. *J. Pharm. Biomed. Anal.* doi:10.1016/j.jpba.2014.02.022.
- 372 Paduano, L., Sartorio, R., Vitagliano, V. and Costantino, L. (1990). Diffusion properties of
373 cyclodextrins in aqueous solution at 25 °C. *J. Sol. Chem.*, 19, 31-39.
- 374 Pavlov, G.M., Korneeva, E.V., Smolina, N.A., and Schubert, U.S. (2010). Hydrodynamic
375 properties of cyclodextrin molecules in dilute solutions. *Eur. Biophys. J.*, 39, 371-379.

- 376 Pessine, F.B., Calderini, A., Alexandrino G.L. (2012). a review: Cyclodextrin inclusion
377 complexes probed by NMR techniques, D.H. Kim (Ed.), Magnetic resonance spectroscopy,
378 InTech Publishing.
- 379 Petersen, M., Simmonds, M.S. (2003). Rosmarinic acid. *Phytochemistry*, 62, 121-125.
- 380 Plasson, R., and Cottet, H. (2005). Determination of homopolypeptide conformational
381 changes by the modeling of electrophoretic mobilities. *Anal. Chem.*, 77, 6047-6054.
- 382 Rocio Campos-Vega, Guadalupe Loarca-Piña, B. Dave Oomah, (2010). Minor components of
383 pulses and their potential impact on human health. *Food Research International*, 43, 461–482.
- 384 Schneider, H., Hacket, F., and Rudiger, V. (1998). NMR Studies of Cyclodextrins and
385 Cyclodextrin Complexes. *Chem. Rev.*, 98, 1755-1785.
- 386 Szejtli, J. (1998). Introduction and general overview of cyclodextrin chemistry. *Chem Rev*, 98,
387 1743-1753.
- 388 Szente, L., Szejtli, J., 2004. Cyclodextrins as food ingredients. *Trends Food Sci. Technol.*, 15,
389 137-142.
- 390 Wang, Y., Qiao, X., Li, W., Zhou, Y., Jiao, Y., Yang, C., Dong, C., Inoue, Y., Shuang, S.
391 (2009). Study on the complexation of isoquercitrin with β -cyclodextrin and its derivatives by
392 spectroscopy. *Analytica Chimica Acta*, 650, 118–123.
- 393 Zhang, M., Li, J., Zhang, L., Chao, J. (2009). Preparation and spectral investigation of
394 inclusion complex of caffeic acid with hydroxypropyl- β -cyclodextrin. *Spectrochimica Acta*
395 *Part A*, 71, 1891–1895.
- 396

397 **Table 1.** Maximal CD-induced ^1H -NMR chemical shift displacements ($\Delta\delta_{\text{max}} = \delta_{\text{max}} - \delta_0$ (no
 398 CD)) of RA protons and binding constant (K_b) at variable pH values in D_2O (RA
 399 concentration = 1 mM).

400

RA proton	pH 1		pH 2.9		pH 6	
	$\Delta\delta_{\text{max}}$ (ppm)	K_b (M^{-1})	$\Delta\delta_{\text{max}}$ (ppm)	K_b (M^{-1})	$\Delta\delta_{\text{max}}$ (ppm)	K_b (M^{-1})
H-2	0.08	320	0.01	265	0.14	209
H-2'	0.08	352	0.06	316	0.012	319
H-5	0.09	314	0.02	260	0.4	256
H-5'	0.03	328	0.03	325	0.03	284
H-6	0.07	300	0.09	260	0.13	202
H-6'	0.09	330	0.06	328	0.02	238
H-7	0.03	342	0.02	313	0.03	222
H-7'	0.05	468	0.03	390	0.04	230
H-8	0.11	466	0.09	393	0.07	227
H-8'	0.11	466	0.08	299	0.07	227

401

402

Figure 1. Chemical structures of (a) β -cyclodextrin (CD) and (b) rosmarinic acid (RA).

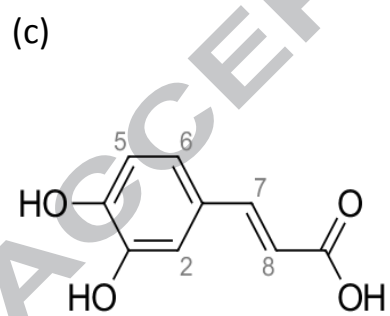
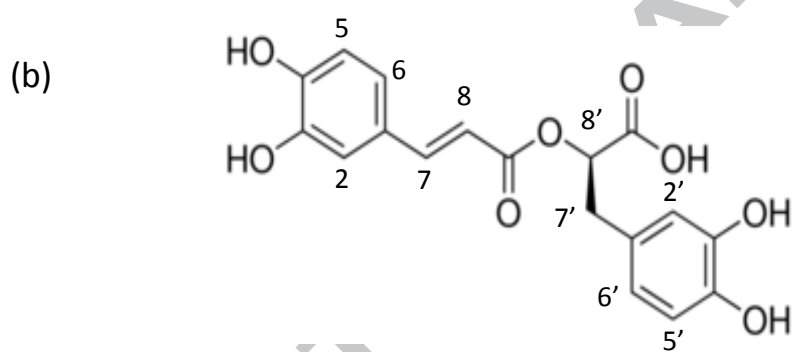
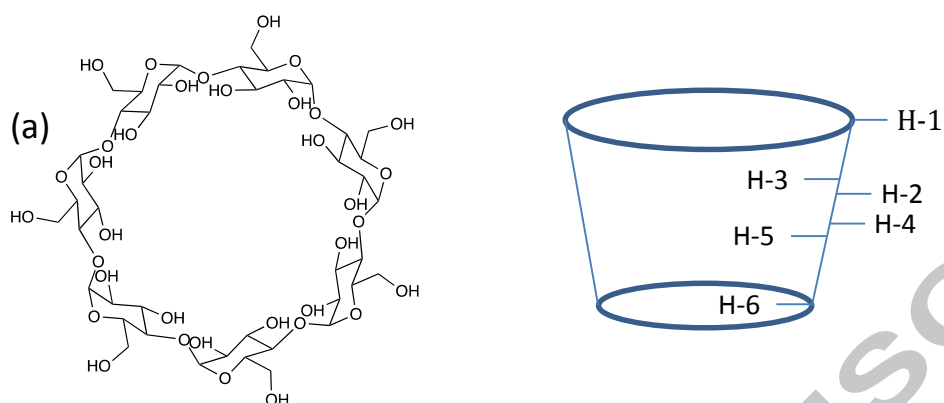


Figure 2. Expansion of the ^1H NMR spectrum showing the displacement of H-5 and H-3 (CD) for a CD mole fraction (r_{CD}) ranging from 0.1 to 0.9 in D_2O at pH 2.9. Different volumes of 10 mM solutions of RA and CD were mixed together to a constant volume keeping the sum of the total RA and CD concentrations equal to 10 mM in D_2O at pH 2.9.

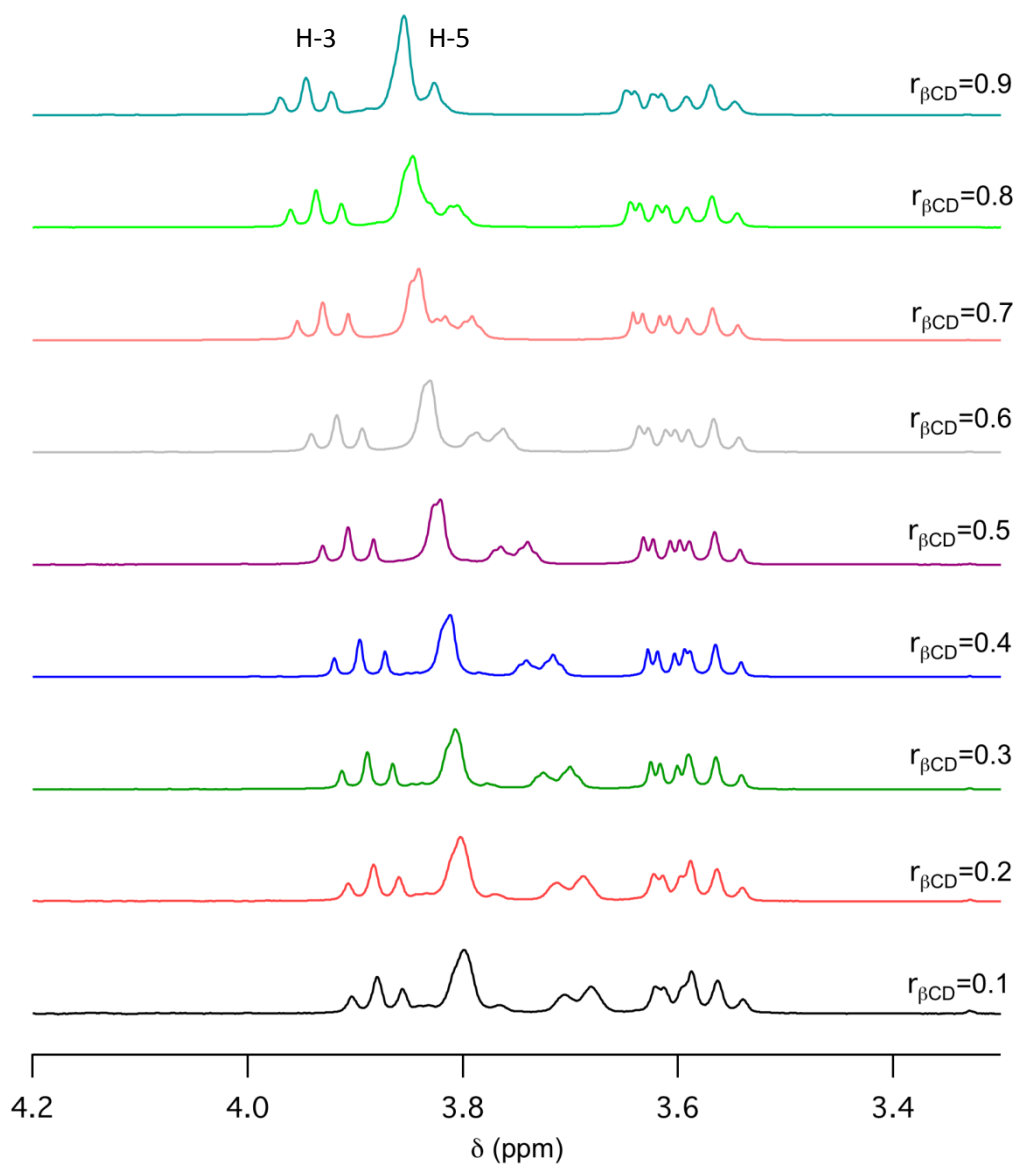


Figure 3. Scott's plot for CD proton H-5 with CD concentration set at 1 mM and variable RA concentration in D₂O at pH 2.9.

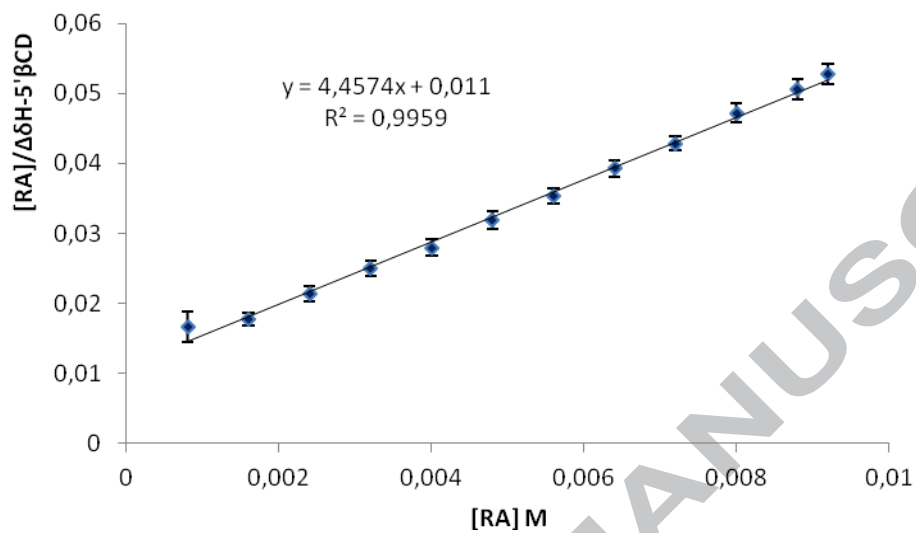


Figure 4. ROESY spectrum of the 1:1 RA-CD complex (5 mM of each partner) in D₂O at pH 2.9 (mixing time = 150 ms).

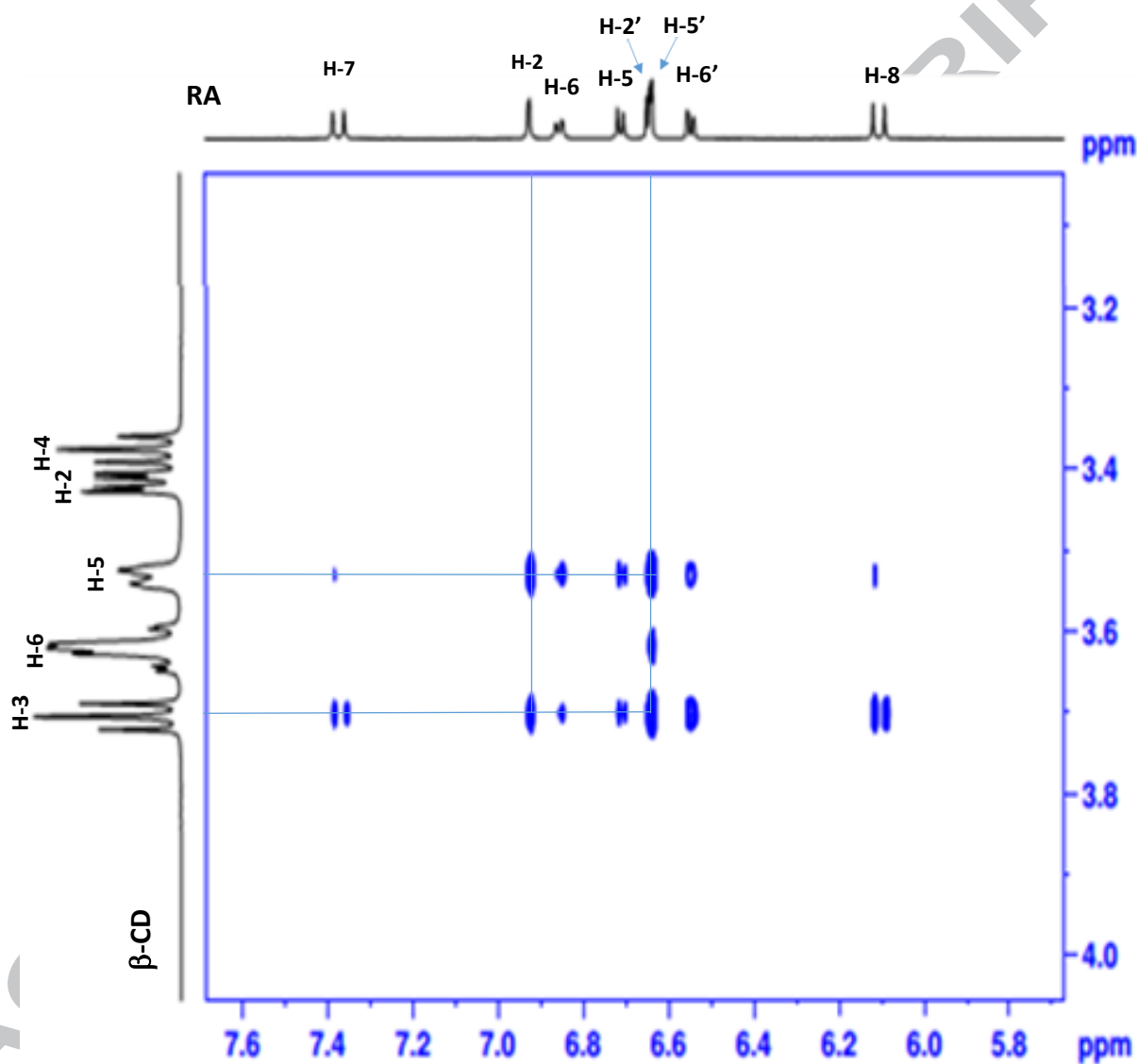
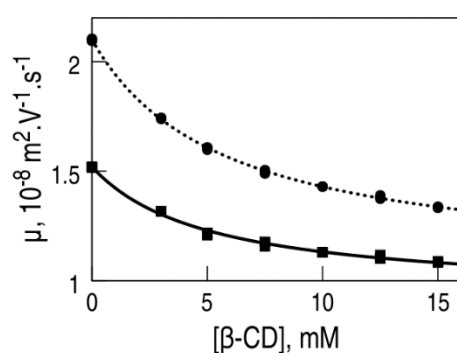


Figure 5. Variation of the electrophoretic mobility of RA (solid line and squares) and CA (dotted line and circles) as a function of the total CD concentration, in phosphate buffer at pH 7, 20 °C, I = 10 mM, [RA] = 0.05 mM, [CA] = 0.2 mM. Circles and squares are experimental measurements for respectively CA-CD and RA-CD, each of them being repeated three times. The lines were obtained by non-linear curve-fitting of experimental data using Eq. 5.



403 **Highlights**

- 404 • Investigation of the RA- β -CD complex by ^1H NMR and CE
- 405 • Estimation of the stoichiometry and binding constant by ^1H NMR
- 406 • Structural analysis of the RA- β -CD complex by ROESY
- 407 • pH dependence of the binding constant
- 408 • Estimation of the binding constants of the RA- β -CD, RA-Me- β -CD and CA- β -CD
- 409 complexes by CE

410

ACCEPTED MANUSCRIPT